# Elevated CO2 levels promote both carbon and nitrogen cycling in global forests

**Gu Baojing**
bjgu@zju.edu.cn
Zhejiang University https://orcid.org/0000-0003-3986-3519
**Jinglan Cui**
Zhejiang University https://orcid.org/0000-0002-8487-0331
**Miao Zheng**
Zhejiang University
**Zihao Bian**
Boston College
**Naiqing Pan**
Boston College
**Hanqin Tian**
Boston College
**Xiuming Zhang**
Zhejiang University
**Ziyue Qiu**
Zhejiang University
**Jianming Xu**
Zhejiang University https://orcid.org/0000-0002-2954-9764

---

**Article**

**Keywords:**

**Posted Date:** September 21st, 2023

**DOI:** https://doi.org/10.21203/rs.3.rs-3336402/v1



**Additional Declarations:** There is **NO** Competing Interest.

**Version of Record:** A version of this preprint was published at Nature Climate Change on April 2nd, 2024. See the published version at https://doi.org/10.1038/s41558-024-01973-9.

# Elevated $CO_2$ levels promote both carbon and nitrogen cycling in global forests

Jinglan Cui[1,2], Miao Zheng[1], Xiuming Zhang[1], Zihao Bian[3,4], Naiqing Pan[3], Hanqin Tian[3], Ziyue Qiu[1], Jianming Xu[1,5], Baojing Gu[1,6*]

[1]College of Environmental and Resource Sciences, Zhejiang University, Hangzhou, 310058, China.
[2]Policy Simulation Laboratory, Zhejiang University, Hangzhou, 310058, China.
[3]Schiller Institute for Integrated Science and Society, Department of Earth and Environmental Sciences, Boston College, Chestnut Hill, MA 02467, USA
[4]School of Geography Science, Nanjing Normal University, Nanjing, 210023, China
[5]Zhejiang Provincial Key Laboratory of Agricultural Resources and Environment, Zhejiang University, Hangzhou, 310058, China.
[6]Ministry of Education Key Laboratory of Environment Remediation and Ecological Health, Zhejiang University, Hangzhou, 310058, China

*Corresponding Author: bjgu@zju.edu.cn (B.G.)

**Forests provide vital ecosystem services, particularly as carbon sinks for nature-based climate solutions. However, the global impact of elevated atmospheric carbon dioxide ($CO_2$) levels on carbon and nitrogen interactions of forests remains poorly quantified. We integrate elevated $CO_2$ experimental observations and biogeochemical cycle model to elucidate the synergies between enhanced nitrogen and carbon cycling in global forests under elevated $CO_2$. Elevated $CO_2$ levels alone increase net primary productivity by 26% (95% CI, 21-30%) and leaf C:N ratio by 32% (18-46%), while stimulating biological nitrogen fixation by 72% (27-136%) and nitrogen use efficiency by 22% (8-38%). Under the elevated $CO_2$ middle road scenario for 2050, forest carbon sink is projected to increase by 0.32 billion tonnes (PgC), with forest products increasing by 4 million tonnes (Tg) nitrogen, reactive nitrogen loss to the environment decreasing by 8 Tg, and fertilizer input decreasing by 4 Tg nitrogen relative to the baseline scenario. The monetary impact assessment of the direct elevated $CO_2$ impact on forests represents a social value of US$292 billion. These findings should inform the development of forest management strategies for future climate change adaptation and mitigation.**

Forests cover approximately 31% of the Earth's land area and serve as habitats for a diverse range of wildlife[1]. They play a crucial role as natural assets that support the livelihoods of 1.6 billion people, particularly those vulnerable segments of society residing in or near forested regions[2]. Forests provide essential ecosystem services to humanity, including forest production, water and soil conservation, as well as carbon capture and storage[3,4]. Specifically, forest ecosystems have the potential to act as carbon sinks, contributing to nature-based decarbonization solutions for combating climate change, and helping offset anthropogenic carbon emissions from agriculture and industrial sectors to achieve Net-Zero emissions[5,6].

The unprecedentedly high levels of $CO_2$ in the atmosphere have driven anthropogenic climate change while also influencing the biophysiological and biogeochemical processes of forest ecosystems, such as stimulating plant growth and productivity through the $CO_2$ fertilization effect[7]. The terrestrial carbon sink has more than doubled in the past five decades largely attributing to the $CO_2$ fertilization[8,9]. The altered carbon stock capacity highly depends on nitrogen availability, and thus, the responses of the nitrogen cycle in the context of climate change might determine whether forests act as carbon sinks or sources[10,11]. The alteration of carbon and nitrogen interactions in forests under elevated $CO_2$ is subject to debate. Some forests could be nitrogen-limited ecosystems, leading to progressive nitrogen limitation under $CO_2$ enrichment[12,13]. Whereas, a recent long-term field study indicates that nitrogen limitation may not occur due to increased litterfall turnover and nitrogen resorption, which sustain the $CO_2$ fertilization effect in an alpine forest.[14].

Globally, nearly one-third of forests are managed primarily for the production of wood and non-wood products[1]. In recent years, increasing nitrogen deposition, combined with human application of synthetic fertilizer, has led to higher nitrogen inputs and associated reactive nitrogen ($N_r$) loss in some forests[15]. However, the specific impact of elevated $CO_2$ as a key driver of climate change on forest nitrogen cycling and $N_r$ loss, is still not well understood and quantified in global forests. The representation of the nitrogen cycle and nitrogen loss ($N_r$ loss) in current Earth System Models has been insufficient, particularly in relation to accounting for the responses of the nitrogen cycle to climate change[16]. It is essential to incorporate the feedback of carbon and nitrogen cycles, along with their interactive processes, into forest management policy-making, for both adapting to and mitigating the impacts of future climate change[17].

In this study, we aim to identify the impacts of elevated $CO_2$ on carbon and nitrogen cycles using a global dataset of elevated $CO_2$ experiments conducted in forests. Subsequently, we propose a modelling framework by integrating the impact of elevated $CO_2$ experiments on carbon and nitrogen cycles with the global forest carbon and nitrogen budgets simulated by the Dynamic Land Ecosystem Model (DLEM)[18] and Coupled Human and Natural Systems (CHANS) model[19]. The integration allows us to project the spatial-temporal variations in forest carbon and nitrogen budgets in response to elevated $CO_2$ under multiple future scenarios. Finally, we conduct a monetary impact assessment of the elevated $CO_2$ on the carbon and nitrogen cycles in global forests, evaluating its economic implications for human society.

**Impact of elevated $CO_2$ on forest carbon and nitrogen cycling**

The impact of elevated $CO_2$ on forest carbon and nitrogen cycles was investigated using a global forest dataset of elevated $CO_2$ experiments. The elevated $CO_2$ experiments, including Free-Air $CO_2$ Enrichment (FACE), Open-Top Chambers (OTC), and Greenhouse Chambers (GC), have been conducted at various forest sites across North America, Central America, Europe, Asia, and Oceania (Fig. 1a). A total of 1,059 response ratios of site-based observations were analyzed to form this global dataset. Globally, elevated $CO_2$ profoundly enhances the carbon cycle, as reflected in promoted plant productivity, plant biomass, soil respiration, and carbon content. Plant net primary productivity (NPP) shows an overall increase of 26% (95% CI: 21-30%, hereinafter) under elevated $CO_2$ (Fig. 1b), with the response sensitivity decreasing as the squared mean annual precipitation (MAP) increases (Fig. S2a). This might be attributable to the reduced stomatal conductance and transpiration under elevated $CO_2$, resulting in higher water use efficiency (+114%, 73-149%) (Fig. S3a) that could ameliorate drought stress and further promote photosynthesis, especially in arid or semi-arid areas[20]. The biomass of different plant components also exhibits distinct increases due to elevated $CO_2$, including leaf biomass (+24%, 16-33%), stem biomass (+24%, 16-33%), and root biomass (+46%, 38-55%) (Fig. 1b). Simultaneously, soil respiration (Rs, soil $CO_2$ emissions from plant roots and microbes) increases by 28% (23-33%). Furthermore, elevated $CO_2$ stimulates soil organic carbon (SOC) (+5%, 1-8%), dissolved organic carbon (DOC) (+16%, 3-34%), and soil microbial biomass carbon (MBC) (+19%, 12-26%).

Meanwhile, elevated $CO_2$ levels induce a 72% increase in rates of biological nitrogen fixation (BNF) (27-136%), and a 24% increase in denitrification rates (4-53%) (Fig. 1b), suggesting a higher microbial capability to transform inert $N_2$ into plant-available nitrogen and to reduce nitrate to $N_2$ under $CO_2$ enrichment. These increases likely result from the stimulated activities of nitrogen-cycling relevant microorganisms, induced by the greater availability of carbon[21]. The improved nitrogen use efficiency (NUE) (+22%, 8-38%) under $CO_2$ enrichment is associated with reduced loss of $N_r$, as nitric oxide ($NO_x$) emissions decrease by 28% (4% to 46%), and leaching and runoff nitrate ($NO_3^-$) decrease by 39% (9% to 60%). Moreover, elevated $CO_2$ leads to decreases in nitrogen concentration of vegetation organisms, such as leaves by 13% (10% to 15%), stems by 7% (2% to 13%), and roots by 8% (1% to 15%) (Fig. 1b). Generally, the accelerated nitrogen cycle, including higher nitrogen input and nitrogen transformation would sustain the $CO_2$ fertilization effect on plant productivity.

Overall, our findings indicate a synergistic enhancement in both the carbon and nitrogen cycles in global forests under elevated $CO_2$ levels, accompanied by shifts in carbon-to-nitrogen (C:N) stoichiometry. The C:N ratios increase in leaves by 32% (18-46%) and in soil by 5% (1-9%) due to elevated $CO_2$ (Fig. 1b). Elevated carbon inputs facilitate nitrogen cycling, while accelerated nitrogen cycling and alleviation of nitrogen limitation, in turn, benefits carbon cycling.

**Global variations of carbon and nitrogen budgets under elevated $CO_2$**

We utilize the DLEM[18] and CHANS[19] models to deliver a plausible global gridded model of forest carbon and nitrogen budgets (Fig. S1). By incorporating the impacts of elevated $CO_2$ experiments on carbon and nitrogen cycles into the parameterization optimization of model simulation, we project the carbon sinks and nitrogen budgets in global forests under multiple future scenarios. Different levels of socioeconomic development and climate change are hypothesized based on the Shared Socioeconomic Pathways (SSPs) and Representative Concentration Pathways (RCPs). The future atmospheric $CO_2$ concentrations are derived from CMIP6 models, leading to the formulation of the $eCO_2$ SSP1-2.6 (SSP1-RCP2.6, "Sustainable society" under elevated $CO_2$ levels) and $eCO_2$ SSP2-4.5 (SSP2-RCP4.5, "Middle road" under elevated $CO_2$ levels), along with the baseline scenarios (SSP1, SPP2, no-climate-change under fixed $CO_2$ levels)[22]. Our results indicate that, in the $eCO_2$ SSP2-4.5 scenario, by the year 2050, forest carbon sink (net biome productivity) is projected to increase by 0.32 billion tonnes (Pg C $yr^{-1}$), while the total nitrogen inputs are projected to increase by 13 million tonnes (Tg N $yr^{-1}$) (Fig. 2). The increased nitrogen input deriving from promoted BNF under elevated $CO_2$ could help sustain the nitrogen demand of the enhanced carbon sink in forests. Additionally, nitrogen in global forest products is expected to increase by 4 Tg N $yr^{-1}$, accumulation nitrogen in biomass and soil is estimated to increase by 19 Tg N $yr^{-1}$, $N_r$ losses are projected to decrease by 8 Tg N $yr^{-1}$, and NUE is projected to increase from 65% to 79% in global forests.

Notably, the global forest carbon sink is projected to rise from 1.05 ± 0.32 Pg C $yr^{-1}$ in the baseline SSP2 scenario to 1.37 ± 0.41 Pg C $yr^{-1}$ in the $eCO_2$ middle road (SSP2-4.5) scenario by the year 2050. This enhanced carbon sink indicates a greater potential for future carbon sequestration and decarbonization capabilities within forest ecosystems, particularly under higher atmospheric $CO_2$ levels compared to current levels. In specific geographical contexts, substantial enhancements in carbon sinks are foreseen in pivotal zones like the tropical forests of the Amazon, the Congo Basin, Southeast Asia, and certain regions of northern Australia (Fig. 2a-c), renowned for their designation as land carbon sink hotspots[23,24].

Under $eCO_2$ middle road scenario, the projected increase of 13 Tg N $yr^{-1}$ in total nitrogen input changes is the sum of the altered various input sources, including BNF (+19 Tg N $yr^{-1}$), deposition (-1 Tg N $yr^{-1}$), and fertilizer (-4 Tg N $yr^{-1}$) in 2050 (Fig. 3). The changes in natural sources of annual nitrogen input include BNF increases from 66 Tg ± 23 N to 84 ± 38 Tg N, while nitrogen deposition slightly decreases from 21 ± 7 Tg N to 19 ± 9 Tg N. Regionally, the largest increases of BNF occur in tropical and subtropical forest, particularly the rainforests in Amazon, the Congo Basin, Southeast Asia, and parts of northern Australia (Fig. S4a-c). The rest of the areas, mainly the temperate and boreal forests, experience slight increments of BNF under elevated $CO_2$. The reductions of nitrogen deposition are dominant in the vast global area, except for occasional minor increases in some regions (Fig. S4d-f). The application of nitrogen fertilizer occurs mainly in some managed forests in the United States, Europe, Asia, and Oceania (Fig. S4g-i). Due to the significant increases in BNF and NUE, which could meet the nitrogen demands of ecosystems, the human source of fertilizer is proposed to reduce from 4 ± 1 Tg N $yr^{-1}$ to zero. In sum, the largest increases of total nitrogen input occur in tropical and subtropical forests (Fig. 2d-f). Boreal forests experience slightly increased nitrogen input at the high latitude in North America and Eurasia, relative to the slightly decreased nitrogen input in some temperate forests in western and eastern parts of North America, western and central Europe, and East Asia. The distinct pattern of variations in total nitrogen inputs across regions depends on the trade-offs among changing BNF, deposition and fertilizer in different types of forest by climatic domains. For instance, the increased nitrogen in tropical forests is dominated by the profoundly increased BNF, much higher than the summed reduction of nitrogen deposition and fertilizer.

The global aggregated nitrogen in forest products increases from 22 ± 4 Tg N $yr^{-1}$ in the baseline SSP2 scenario to 26 ± 6 Tg N $yr^{-1}$ in the $eCO_2$ middle road scenario for 2050. The forest products, including wood and non-wood products, originate from some forests in all the continents, apart from the intact forests without any human interventions (Fig. 2g-i). Increases in forest products are mainly projected in wood production hotspots such as Europe, Eastern Asia, North America, southeastern Latin America, and parts of Sub-Sahara Africa[1]. Additionally, nitrogen accumulation in the living biomass and soil stock increases from 37 ± 14 Tg N $yr^{-1}$ to 56 ± 17 Tg N $yr^{-1}$ due to elevated $CO_2$ (Fig. S5a-c). The majority of increases in accumulation occur in tropical and subtropical forests, followed by boreal forests, suggesting that increased nitrogen input dominates these regions. On the other hand, minor decreases in accumulation take place in temperate forests in Europe, western North America, and Northeastern Asia, where intensive production activities might be responsible for depleting the nitrogen pool[25].

The $N_r$ losses all exhibit a decreasing trend in the $eCO_2$ middle road scenario for 2050, with reductions in $NH_3$ (-0.8 Tg N $yr^{-1}$), $N_2O$ (-0.9 Tg N $yr^{-1}$), $NO_x$ (-1.2 Tg N $yr^{-1}$), and $NO_3^-$ (-5 Tg N $yr^{-1}$), respectively (Fig. 3). Regionally, the most significant reductions in aggregated $N_r$ losses are projected in northern South America, central Africa, South and Southeast Asia, and parts of northern Australia (Fig. 2j-l). For the specific $N_r$ component, reductions in $NH_3$ emissions are dominant in most areas, with profound reductions in parts of North America, Europe, and East Asia (Fig. S6a-c). The spatial reductions in $N_2O$ emissions are similar to that of $NO_x$ emissions (Fig. S6d-i). Slight increases in $N_2O$ and $NH_3$ emissions occur in certain intact tropical and boreal forests due to the significant increase in nitrogen input from higher BNF. The reductions in $NO_3^-$ leaching and runoff to water bodies are most substantial, especially in the tropical and subtropical forests in Amazon, Congo Basin, Asia, and North Australia, followed by the temperate forests in eastern North America, Europe, and Northeast Asia (Fig. S6j-l).

**Multiple scenario analysis and impact assessment**

Monte Carlo simulations were employed to estimate the averages and uncertainty ranges of nitrogen budget during the study period from 2000 to 2050 (Fig. 4). Historical data indicates that the global forest area has remained relatively stable with a slight downward trend in recent two decades. In the projection beyond 2020, the global forest area is expected to expand over time due to anticipated afforestation and reforestation in the baseline SSP1 "Sustainable society" scenario; conversely, the forest area is projected to shrink due to potential deforestation resulting from human interventions in the baseline SSP2 "Middle road" scenario[26]. The forest area in SSP1 is greater than that in SSP2, and the forest area is correlated with the size of the nitrogen budget, thus leading to higher baseline carbon sinks, nitrogen inputs, forest products, and $N_r$ losses in SSP1 compared to SSP2 at the same time point. Both elevated $CO_2$ SSP1-2.6 and SSP2-4.5 scenarios show consistent effects on forest carbon and nitrogen budgets. These effects include increased carbon sinks, enhanced total nitrogen inputs, higher forest product yields, and reduced $N_r$ losses under the $eCO_2$ scenarios in comparison to their corresponding baseline scenarios. This suggests that the positive impacts of elevated $CO_2$ on carbon-nitrogen interactions remain robust across diverse socioeconomic and climate scenarios spanning from 2030 to 2050. Using the SSP1-2.6 scenario as an illustration, elevated $CO_2$ is projected to increase carbon sink from $1.58 \pm 0.24$ Pg C $yr^{-1}$ to $2.06 \pm 0.31$ Pg C $yr^{-1}$, boost nitrogen input from $144 \pm 19$ Tg N $yr^{-1}$ to $162 \pm 20$ Tg N $yr^{-1}$, raise forest products from $29 \pm 4$ Tg N $yr^{-1}$ to $34 \pm 4$ Tg N $yr^{-1}$, and decrease $N_r$ losses from $32 \pm 4$ Tg N $yr^{-1}$ to $18 \pm 7$ Tg N $yr^{-1}$ by the year of 2030.

Subsequently, we undertake a comprehensive economic assessment to gauge the direct impacts of elevated $CO_2$ on the forest carbon and nitrogen cycles under $eCO_2$ middle road scenario. Our evaluation isolates elevated $CO_2$ as the sole driver of climate change, bypassing the consideration of other climate change drivers like warming and altered precipitation regimes. The economic valuation of the societal benefits amounts to US$292 billion, encompassing diverse aspects of human health benefits (US$17 billion), ecosystem benefits (US$44 billion), climate impacts (US$17 billion), and forest production (US$213 billion) (Fig. 5). Foremost among these benefits is forest production, making a substantial contribution to the overall benefit with a noteworthy surge of US$211 billion in forest product revenues, along with a US$2 billion reduction in fertilizer input expenses. The second-highest benefit stems from climate impact, encompassing a US$10 billion benefit arising from carbon sequestration, coupled with an additional US$7 billion derived from $N_r$-induced climate impact (i.e., the reduction of $N_2O$ emissions and its subsequent decrease in global warming potential). Human health and ecosystem benefits primarily result from the reduction of $N_r$ emissions, thereby avoiding harm to both humans and the ecosystem health. Among various geographical regions, North America, including Canada and the United States, stands out as the primary beneficiary, accumulating benefits totaling US$56 billion. Europe closely follows with US$51 billion, and China secures the third position with benefits amounting to US$48 billion.

**Future perspective**

Accelerated carbon and nitrogen cycles in forests create potential synergies that offer opportunities to enhance forest production, carbon sequestration, and mitigate nitrogen pollution. To harness and optimize these benefits in global forests, it is essential to recognize the changes in the coupled carbon-nitrogen relationship and develop sustainable forest production in the context of future climate change.

Our study projects that elevated $CO_2$ will benefit forest carbon cycling by promoting forest productivity and increasing the living biomass stock. Increased nitrogen input from natural sources, aided by BNF, helps sustain $CO_2$ fertilization effects on forest growth and productivity. This reduces the need for synthetic fertilizer in nitrogen-limited natural forests and plantations.

The net incomes from forest production are likely to increase, given the higher yields of forest products and the lower cost of fertilizer. As forest production provides livelihoods for the population residing in impoverished mountainous regions[2], the increased incomes of producers could directly contribute to alleviating poverty and reducing regional inequality.

Moreover, the $CO_2$ fertilization presents an opportunity to expand forest carbon sinks, making a greater contribution to carbon neutrality and the goal of limiting global warming below 2°C or even 1.5°C. Enhancing forest conservation, restoration, and afforestation efforts can facilitate and maximize the realization of this potential. This involves implementing ecological restoration projects to expand forested areas and selecting tree species adapted to high atmospheric $CO_2$ concentrations and possessing high carbon density[17,27]. Meanwhile, global warming and altered precipitation regimes along with $eCO_2$ would also change the future distribution of forest, and global forest carbon and nitrogen cycles[28–30]. This would require further efforts from integrated studies in the context of climate change.

Additionally, the altered carbon-nitrogen interactions under elevated $CO_2$ demand optimized forest nutrient management. Nitrogen fertilizer usage should be adjusted, and fertilization strategies optimized based on soil nutrient dynamics to improve NUE and reduce production costs. This practice helps mitigate excess $N_r$ losses to the environment and the associated nitrogen pollution, ultimately yielding ecosystem and health benefits for society as a whole[31]. Furthermore, our study is subject to uncertainties arising from data sources and modeling procedures. Future efforts are required to narrow down these ranges of uncertainty. Additional field manipulation experiments in tropical forests are essential to gather firsthand observations on how climate change modulates biogeochemical cycles, which can help fill the data gaps in tropical regions. Further research is needed to examine the responses of other nutrient element balances, aside from nitrogen, to climate change. Field studies have indicated that phosphorus limitation can influence plant productivity responses to elevated $CO_2$ and warming in natural ecosystems[32,33]. Maintaining a balanced stoichiometry of nutrient elements, including phosphorus (P) and potassium (K), is crucial for preserving the health and service functions of forest ecosystems.

## Methods

### Database of elevated $CO_2$ experiments in forests and global synthesis

Data from elevated $CO_2$ experiments (listed in Supplementary Information Table S1) and additional sources were compiled to create a comprehensive global dataset on elevated $CO_2$ in forest ecosystems. Our selection criteria ensured the inclusion of qualified studies, which met the following criteria: (1) experiments with control (ambient $CO_2$) and treatment (elevated $CO_2$) groups; (2) regular measurements of variables related to nitrogen and carbon cycles; (3) studies published in peer-reviewed journals and indexed in authoritative databases such as Web of Science, Google Scholar, and Scopus. Site locations, experimental settings, and variable information were extracted from text, tables, and figures. Data from figures were extracted using WebPlotDigitizer 4.4 (https://apps.automeris.io/wpd/). In addition, climate data, soil texture, and climate zones were compiled from external sources. Climate data for study sites were obtained from the WorldClim database using site coordinates (https://worldclim.org/data/index.html#). Soil texture information was derived from the Global Land Data Assimilation System (GLDAS) (https://ldas.gsfc.nasa.gov/gldas/soils). Climate zones were assigned based on the Köppen-Geiger climate classification[34].

For the global synthesis of response mechanisms to elevated $CO_2$ levels, we employed multi-level meta-analyses across four levels: (i) individual observations, (ii) combinations by climate zones (e.g., cold, temperate, arid, tropical), (iii) global scale.

To calculate the response ratio of an individual observation, we used the natural logarithm of the response ratio (*lnR*) formula[35], as follows:

$$lnR = \ln \frac{x_{eCO_2}}{x_{aCO_2}} \tag{1}$$

where $x_{eCO_2}$ and $x_{aCO_2}$ represent the means of parameters at elevated $CO_2$ levels and ambient $CO_2$, respectively.

The weight of each individual observation was determined based on the number of experimental replications:

$$Weight = \frac{n_{eCO_2} \times n_{aCO_2}}{n_{eCO_2} + n_{aCO_2}} \tag{2}$$

where $n_{eCO_2}$ and $n_{aCO_2}$ denote the number of replications at elevated $CO_2$ levels and ambient $CO_2$ levels, respectively.

Subsequently, we acquired weighted mean response ratios (*RR*) at various levels, accompanied by 95% confidence intervals, utilizing a randomized resampling procedure through bootstrapping over 4,999 iterations with *MetaWin 2.0*[36]. A significant response ratio ($P<0.05$) was indicated by non-overlapping 95% confidence intervals with zero.

The results were reported as percentage changes of response ratios (*RR*%) for clarity.

$$RR\% = (e^{RR}-1) \times 100\% \tag{3}$$

To explore the spatial heterogeneity of response patterns, we conducted meta-regressions for each variable with potential moderators using the *metafor* package in the *R* platform (version 4.1.3)[37]. The moderators considered include manipulation magnitude ($\Delta CO_2$), mean annual temperature (*MAT*), mean annual precipitation (*MAP*), maximum temperature, minimum temperature, soil texture, and others (Fig. S2).

## Global forest carbon and nitrogen budgets

The global gridded carbon and nitrogen budgets for forests were estimated using the DLEM[18] and CHANS[19] models at a spatial resolution of 0.5° × 0.5° (Fig. S1).

DLEM is a dynamic global vegetation model that simulates the daily cycles of carbon, water, and nitrogen driven by atmospheric chemistry, climate, land-use changes, and disturbances[18].

The calculation of plant net primary productivity (*NPP*) at the grid *i* level is based on the following equations:

$$NPP_i = GPP_{sun,i} + GPP_{shade,i} - G_{r,i} - M_{r,i} \tag{4}$$

$$G_{r,i} = 0.125(GPP_{sun,i} + GPP_{shade,i}) \quad (5)$$

$$GPP_{sun,i} = 12.01 \times 10^{-6} \times A_{sun,i} \times LAI_{sun,i} \times dayl_i \times 3600 \quad (6)$$

$$GPP_{shade,i} = 12.01 \times 10^{-6} \times A_{shade,i} \times LAI_{shade,i} \times dayl_i \times 3600 \quad (7)$$

where $GPP_{sun}$ and $GPP_{shade}$ represent gross primary productivity (*GPP*) of sunlit and shaded canopy, respectively (g C/m$^2$/d); *Gr* denotes the growth respiration of plants (g C/m$^2$/d); $A_{sun}$ and $A_{shade}$ are leaf level assimilation rates of sunlit and shaded canopy, respectively (μmol $CO_2$/m$^2$/s); $LAI_{sun}$ and $LAI_{shade}$ are projected leaf area index of sunlit and shaded canopy, respectively (fraction); *dayl* is daytime length (hour) in a day; $12.01 \times 10^{-6}$ is a constant to change the unit from μmol $CO_2$ to g C.

Maintenance respiration (*Mr*) of plants (g C/m$^2$/d) is a function of surface air temperature and biomass carbon content, including carbon pools in different plant parts (i.e., leaf, sapwood, fine root, and coarse root). The calculation of Mr is performed by summarizing all plant parts as follows:

$$M_{r,i} = \sum(\min(Rsep_{coef} \times f(T), r_{max}) \times CV_m) \quad (8)$$

where $Rsep_{coef}$ is a plant functional type specific respiration coefficient; *f(T)* is the temperature factor, calculated as a function of daily average air temperature; $r_{max}$ is the maximum respiration rate of different carbon pools; *CVi* is the carbon content (g C/m$^2$) of vegetation pool *m*.

DLEM has 6 vegetation pools, 8 soil pools, 6 litter pools, and 3 product pools. The calculation of annual net biome productivity at time *t* is based on the following equation:

$$NBP_t = (CV_t + CS_t + CL_t + CP_t) - (CV_{t-1} + CS_{t-1} + CL_{t-1} + CP_{t-1}) \quad (9)$$

where $NBP_t$ is net biome productivity at time *t;* $CV_t$, $CS_t$, $CL_t$, $CP_t$ are the carbon content (g C/m$^2$) of vegetation pool, soil pool, litter pool, and product pool at time *t*, respectively; $CV_{t-1}$, $CS_{t-1}$, $CL_{t-1}$, $CP_{t-1}$ are the carbon content (g C/m$^2$) of vegetation pool, soil pool, litter pool, and product pool at time *t-1*, respectively.

CHANS stands as a nitrogen cycle model that simulates nitrogen flows within diverse interlinked subsystems of the natural-human interface[19,38]. These subsystems encompass cropland, grassland, forest, atmosphere, surface water, and groundwater. Our study concentrates specifically on the forest subsystem.

The calculation of forest nitrogen budget is carried out at the grid *i* level based on the N mass balance principle. The key nitrogen parameters, including nitrogen input ($N_{input,i}$), $N_r$ ($N_{r,i}$), forest products ($N_{products,i}$), forest accumulation ($N_{accumulation,i}$), and NUE ($NUE_i$), are identified using the following equations:

$$\sum_1^k N_{input,i} = \sum_1^k N_{r,i} + \sum_1^k N_{2,i} + \sum_1^k N_{products,i} + \sum_1^k N_{accumulation,i} \quad (10)$$

$$\sum_1^k N_{input,i} = \sum_1^k N_{BNF,i} + \sum_1^k N_{deposition,i} + \sum_1^k N_{fetilizer,i} \quad (11)$$

$$\sum_1^k N_{r,i} = \sum_1^k NH_{3,i} + \sum_1^k N_2O_i + \sum_1^k NOx_{,i} + \sum_1^k NO_3^-{}_i \quad (12)$$

$$NUE_i = \frac{N_{products,i} + N_{accumulation,i}}{N_{input,i}} \quad (13)$$

where $N_{input,i}$ represents the total N input, consisting of BNF ($N_{BNF,i}$), N deposition including both wet deposition (rainfall and snow) and dry deposition (direct settling of particles and gases) ($N_{dep,i}$), and synthetic fertilizer ($N_{fer,i}$); reactive nitrogen ($N_{r,i}$) includes $NH_3$ emissions ($NH_{3,i}$), $N_2O$ emissions ($N_2O_i$), $NO_x$ emissions ($NO_{x,i}$), and N leaching and runoff to water ($NO_{3,i}^-$); $N_{2,i}$ denotes $N_2$ emissions; $N_{products,i}$ represents the quantity of N in both wood and none-wood forest products; $N_{accumulation,i}$ denotes the N increment in living biomass, litterfall, and soil stock.

The emission factor ($F_{emit,i}$) are defined as:

$$F_{emit,i} = \frac{N_{emit \cdot component,i}}{N_{surplus,i}} \quad (14)$$

where $N_{emit\ component,i}$ could be any component of $N_{r,i}$, such as $N_{NH_{3,i}}$, $N_{N_2O_i}$, $N_{NO_{x,i}}$, and $NO_{3,i}^-$.

In this study, we adopt a multi-model simulation approach to establish robust global forest carbon and nitrogen budgets, effectively mitigating uncertainties. The gridded data generated by the DLEM is systematically integrated into the CHANS model. This integration involves a comparison and calibration process with the nationally-scaled data embedded within the CHANS model, generating a finely-detailed and accurate gridded dataset.

**Scenario design and model simulation**

In this study, we developed two sets of scenarios: (i) Baseline scenarios, representing no-climate-change conditions, consist of SSP1 ('Sustainable society') and SSP2 ('Middle road'); (ii) $eCO_2$ scenarios, encompassing SSP1-2.6 ('Sustainable society') and SSP2-4.5 ('Middle road'), consider elevated $CO_2$ levels as the sole driver of climate change. The future atmospheric $CO_2$ concentrations were derived from CMIP6 models[22]. Additionally, the future forest areas under different socio-economic pathways (SSP1 and SSP2) were projected based on a Global Change Analysis Model for future land use[26].

Next, we conducted a multi-model simulation under various scenarios. The impact of elevated $CO_2$ on plant NPP and stem nitrogen content is integrated into the forest products within grid *i* as below:

$$N_{products,i}^{eCO_2} = N_{products,i}^{base} \times (1 + RR\%_{NPP,i}) \times (1 + RR\%_{stem[N],i}) \quad (15)$$

where $N_{products,i}^{eCO_2}$ and $N_{products,i}^{base}$ represent the N in the forest products under the elevated $CO_2$ scenario and baseline scenario, respectively; $RR\%_{NPP,i}$ denotes the response ratio of NPP to elevated $CO_2$; $RR\%_{stem[N],i}$ denotes the response ratio of stem N content to elevated $CO_2$.

The effects of elevated $CO_2$ on NUE are incorporated into the base NUE within grid *i* as follows:

$$NUE_i^{eCO_2} = NUE_i^{base} \times (1 + RR\%_{NUE,i}) \quad (16)$$

where $NUE_i^{eCO_2}$ and $NUE_i^{base}$ represent the NUE under the elevated $CO_2$ and baseline scenarios, respectively; $RR\%_{NUE,i}$ denotes the response ratio of NUE to elevated $CO_2$.

As for the calculation of $N_r$ emissions, the effects of elevated $CO_2$ on $N_r$ are incorporated into the emission factors within grid *i* as follows:

$$F_{emit,i}^{eCO_2} = F_{emit,i}^{base} \times (1 + RR\%_{Nrcomponent,i}) \quad (17)$$

where $F_{emit,i}^{eCO_2}$ and $F_{emit,i}^{base}$ represent the emission factors under the elevated $CO_2$ and baseline scenarios, respectively; $RR\%_{Nrcomponent,i}$ denotes the response ratio of any $N_r$ component to elevated $CO_2$.

The total N input under elevated $CO_2$ ($N_{input}^{eCO_2}$) is obtained by summing up all the N output components within grid *i* as follows:

$$N_{input,i}^{eCO_2} = N_{r,i}^{eCO_2} + N_{2,i}^{eCO_2} + N_{products,i}^{eCO_2} + N_{accumulation,i}^{eCO_2} \quad (18)$$

where $N_{r,i}^{eCO_2}$, $N_{2,i}^{eCO_2}$, $N_{products,i}^{eCO_2}$, and $N_{accumulation,i}^{eCO_2}$ represent the $N_r$, $N_2$, and the N in the forest products and ecosystem accumulation under the elevated $CO_2$ scenario, respectively.

The BNF under the elevated $CO_2$ scenario ($N_{BNF,i}^{eCO_2}$) is attained by integrating the effects of elevated $CO_2$ on the base BNF rates as follows:

$$N_{BNF,i}^{eCO_2} = N_{BNF,i}^{base} \times (1 + RR\%_{BNF,i}) \quad (19)$$

where $N_{BNF,i}^{base}$ represents the BNF under the baseline scenario; $RR\%_{BNF,i}$ denotes the response ratio of BNF to elevated $CO_2$.

The N deposition under the elevated $CO_2$ scenario ($N_{deposition,i}^{eCO_2}$) is attained by integrating the effects of elevated $CO_2$ on the base N deposition as follows:

$$N_{deposition,i}^{eCO_2} = N_{deposition,i}^{base} + \Delta NH_{3,i} + \Delta NO_{x,i} \quad (20)$$

where $N_{deposition,i}^{base}$ represents the deposition under the baseline scenario; $\Delta NH_{3,i}$ and $\Delta NO_{x,i}$ denote the changes of $NH_3$ emissions and $NO_x$ emissions due to elevated $CO_2$, respectively.

The allocation of human-source fertilizer under the elevated $CO_2$ scenario is conducted based on the disparity between the total N input and the natural-source N input, including BNF and N deposition.

The effects of elevated $CO_2$ on carbon contents are incorporated into the NBP as follows within grid *i*:

$$NBP_i^{eCO_2} = \sum (NBP_{i,m}^{base} \times (1 + RR\%_{[C],i,m})) \quad (21)$$

where $NBP_i^{eCO_2}$ represent the NBP under the elevated $CO_2$ scenario; $NBP_{i,m}^{base}$ denotes the NBP of carbon pool *k* under the baseline scenario; $RR\%_{[C],i,m}$ denotes the response ratio of carbon content to elevated $CO_2$ for carbon pool *m*.

**Impact assessment**

The monetary impact analysis of elevated $CO_2$ ($I_{eCO_2}$) as a single climate change driver is conducted at the grid level in global forests, considering its potential impacts on human health ($I_{health}$), ecosystem ($I_{eco}$), climate change ($I_{climate}$), and forest production ($I_{pro}$) within grid *i* as follows:

$$I_{eCO_2,i} = I_{health,i} + I_{eco,i} + I_{climate,i} + I_{pro,i} \quad (22)$$

The human health impact is determined by the altered health damage resulting from varying $N_r$ emissions under elevated $CO_2$ levels within grid *i* as follows[39]:

$$I_{health,i} = \Delta N_{r,i} \times d_{health,i} \quad (23)$$

where $\Delta N_{r,i}$ represents the change in $N_r$ elevated $CO_2$ at grid *i*; $d_{health,i}$ denotes the human health damage cost of $N_r$ , which is calculated based on the metric of N-share to $PM_{2.5}$ pollution.

The ecosystem impact is quantified as the altered damage cost of $N_r$ effects on the ecosystem within grid *i* using the following equation[40,41]:

$$I_{eco,i} = \Delta N_{r,i} \times d_{eco,EU} \times \frac{WTPj}{WTP_{EU}} \times \frac{PPPj}{PPP_{EU}} \quad (24)$$

where $\Delta N_{r,i}$ represents the change in $N_r$ elevated $CO_2$ scenario relative to the baseline, including $NH_3$, $N_2O$, $NO_x$, and $NO_3^-$ losses at grid *i*; $d_{eco,EU}$ stands for the estimated ecosystem damage cost of $N_r$ emission in the European Union (EU) based on the European N Assessment; $WTP_j$ and $WTP_{EU}$ denote the values of the willingness to pay for ecosystem service in the country/ area *j* and the EU, respectively; $PPP_j$ and $PPP_{EU}$ denote the purchasing power parity of the country/ area *j* and the EU. We extend the ecosystem damage cost of $N_r$ emission in the EU to other countries by applying willingness to pay and purchasing power parity adjustments for comparable ecosystem benefits worldwide, due to data limitations.

The assessment of climate impact is conducted considering the influence of carbon sequestration and the $N_r$ losses on climate change within grid *i* as follows[42]:

$$I_{climate,i} = \Delta C_i \times p_{C,i} + \Delta N_{r,i} \times d_{climate,i} \tag{25}$$

where the change in C sequestration under elevated $CO_2$ is estimated by multiplying change of carbon sequestration ($\Delta C_i$) and the carbon price ($p_{C,i}$); we use the national carbon prices for calculation[43], and the missing values for some countries are supplemented with means of the income groups; the influence of $N_r$ losses on climate change is estimated by multiplying change of $N_r$ losses ($\Delta N_{r,i}$) and climate damage cost of $N_r$. The effects of $N_r$ on climate change can be positive or negative, i.e., $N_2O$ contributes to climate warming as a potent greenhouse gas, while $NO_x$ and $NH_3$ exert climate cooling give that they are precursors of aerosol reflecting long-wave solar radiation.

The monetary evaluation of forest production is conducted in terms of production cost (i.e., fertilizer application) and incomes from forest products within grid *i,* as shown in the following equation:

$$I_{pro,i} = \Delta N_{fertilizer,i} \times p_{fertilizer,i} + \Delta N_{pro,i} \times p_{pro,i} \tag{26}$$

where $\Delta N_{fertilizer,i}$ denotes the changes in N fertilizer under elevated $CO_2$; the N fertilizer price ($p_{fertilizer,i}$) is estimated by dividing the value of fertilizers traded by the quantity based on the UN Comtrade Database (https://comtrade.un.org/); where $\Delta N_{pro,i}$ denotes the changes in forest products under elevated $CO_2$; the price of forest products ($p_{pro,i}$) is estimated by dividing the value of forest products traded by the quantity based on the FAO database (https://www.fao.org/faostat/en/#data/FO). For some countries with missing values of price, the global mean value is used as a substitute.

## Uncertainty analysis

To evaluate the uncertainty of our model outputs, we conducted an uncertainty analysis using the CHANS model with Monte Carlo simulations. We performed 1,000 iterations to generate projection ensembles and calculate the average and variability of nitrogen budgets. Coefficients of variation (CV) were utilized to quantify the relative ranges of uncertainty for nitrogen budget data and the effects of warming on nitrogen dynamics (Table S2).

**Correspondence and requests for materials** should be addressed to Baojing Gu.

## Data availability

Data on the main findings can be found in the Supplementary Information.

## Acknowledgments

This study was supported by the National Natural Science Foundation of China (42325707, 42261144001 and 42061124001), and National Key Research and Development Project of China (2022YFE0138200 and 2022YFD1700700).

## Author contributions

B.G. and J.C. designed the study. J.C. analyzed the data and wrote the first draft of the paper.

All authors contributed to the discussion and revision of the paper. M.Z. provided support for data collection and visualization. X.Z. provided support for CHANS model and impact assessment. Z.B., N.P., and H.T. provided modelling support for DLEM. Z.Q. collected data from climate change experiments. J.X. contributed to the discussion of the study.

## Competing interests

The authors declare no competing interests.

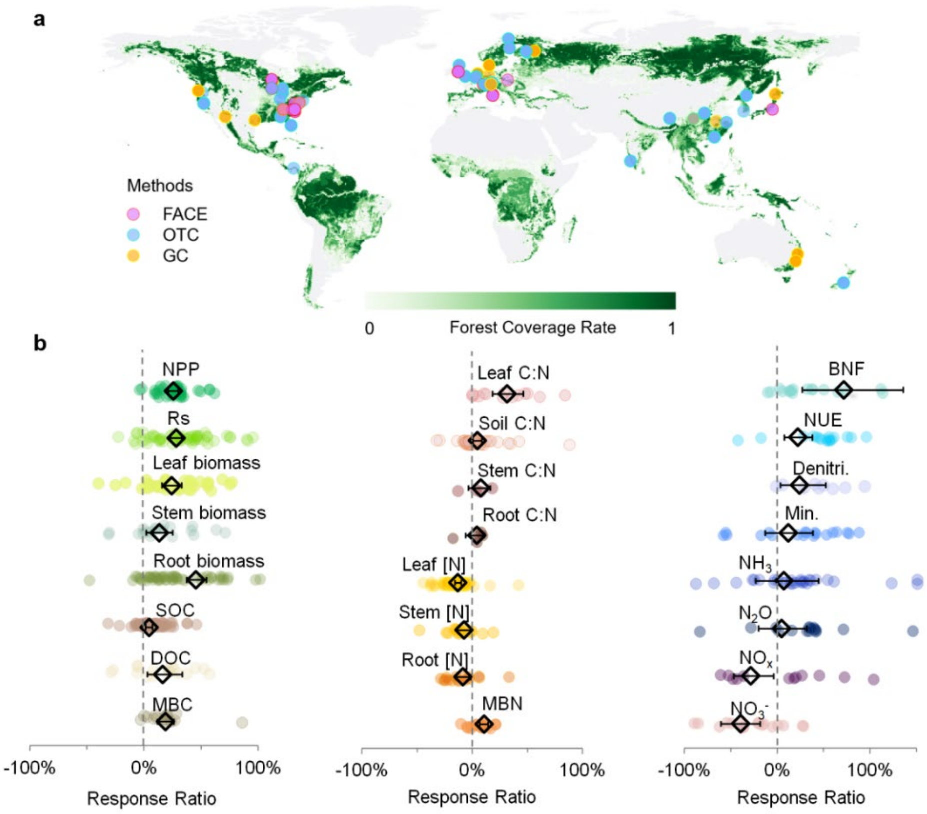


**Fig. 1 | Global elevated $CO_2$ ($eCO_2$) experimental sites and $eCO_2$ impact on carbon and nitrogen variables in global forests. (a)** $eCO_2$ experiments sites with diverse manipulation methods. FACE, Free-Air $CO_2$ Enrichment; OTC, Open-Top Chamber; GC, such as Greenhouse and Growth Chamber. (**b)** Response ratios of key carbon and nitrogen cycling parameters to $eCO_2$ from meta-analysis. Scatter plots represent response ratios of observations, and diamonds with error bars indicate mean values of response ratios with 95% confidence intervals. The value of response ratio is significant if the 95% confidence interval does not overlap zero. NPP, net primary productivity; Rs, soil respiration; SOC, soil organic carbon; DOC, dissolved organic carbon; MBC, microbial biomass carbon; [N], nitrogen content; MBN, microbial biomass nitrogen; BNF, biological nitrogen fixation; NUE, nitrogen use efficiency; Denitri., Denitrification; Min., nitrogen mineralization; $NO_3^-$, leaching and runoff nitrate to water. The base map is applied without endorsement from GADM data (https://gadm.org/).

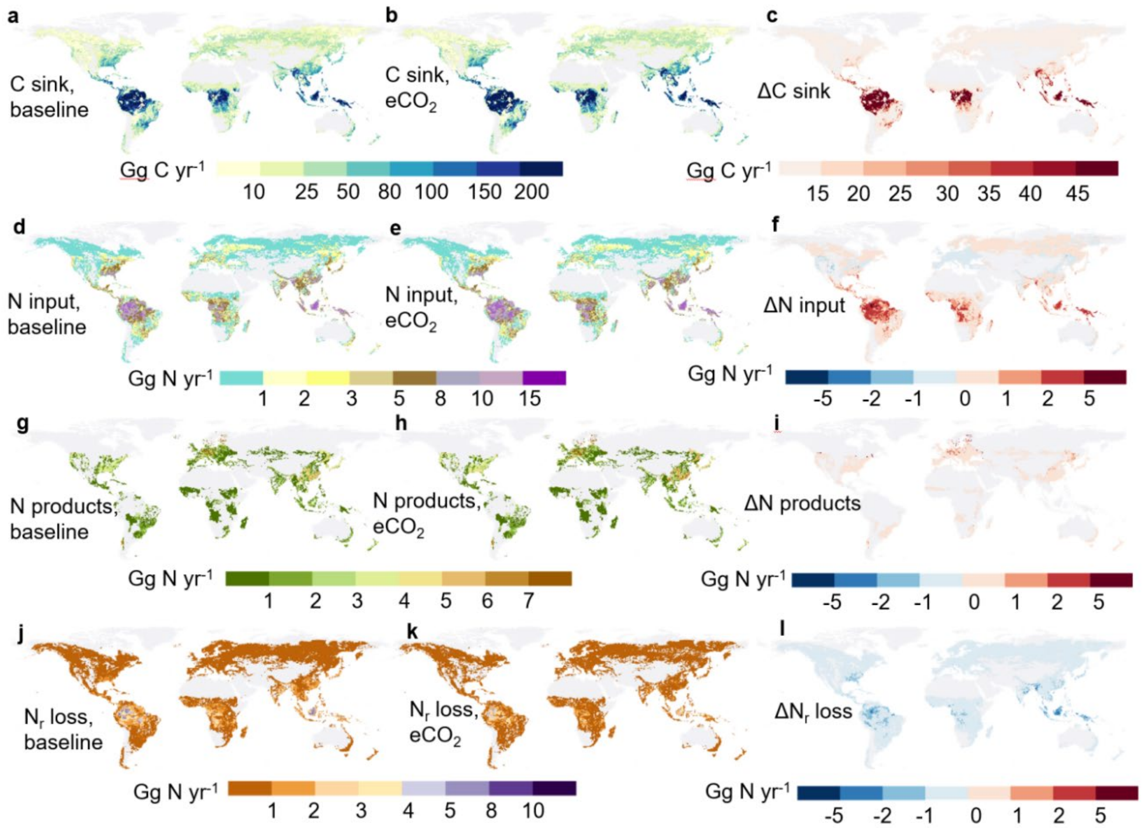


**Fig. 2 | Carbon sink and nitrogen budgets of global forests and their changes between elevated $CO_2$ middle road scenario (SSP2-4.5) and baseline scenario in 2050.** Carbon sink (net biome productivity) in baseline scenario (**a**), $eCO_2$ scenario (**b**), and ΔC sink ($eCO_2$-induced change) (**c**); N input in baseline scenario (**d**), $eCO_2$ scenario (**e**), and ΔN input ($eCO_2$-induced change) (**f**); N products in baseline scenario (**g**), $eCO_2$ scenario (**h**), and ΔN products (**i**); $N_r$ loss in baseline scenario (**j**), $eCO_2$ scenario (**k**), and $\Delta N_r$ loss (**l**). Values in the legend reflect the average annual budgets from forest within a grid cell (0.5° × 0.5°). The base map is applied without endorsement from GADM data (https://gadm.org/).

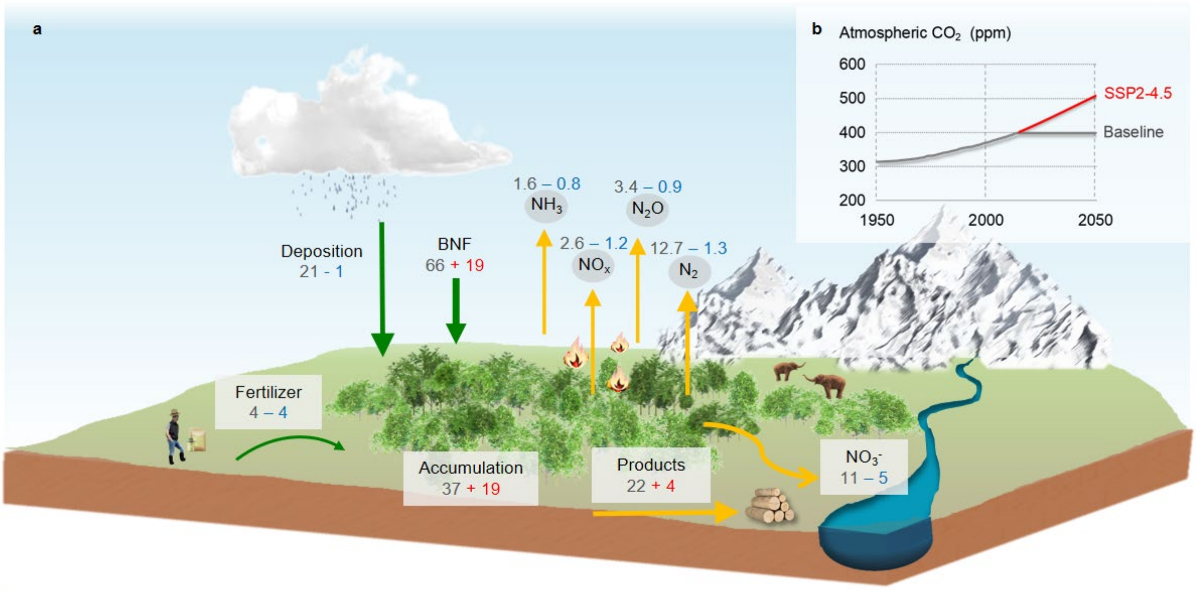


**Fig. 3 | Nitrogen flows in global forests under elevated $CO_2$ middle road scenario (SSP2-4.5) for 2050.** (**a**) Schematic representation of nitrogen budgets in global forests. Green and yellow arrows represent nitrogen input and output, respectively. Accumulation denotes the nitrogen residue in living trees and soil stock. Values of nitrogen flows in dark grey represent flows in the baseline scenario, with the red or blue values indicating increases or decreases in nitrogen flows due to elevated $CO_2$. The unit is Tg N $yr^{-1}$. (**b**) Historical and future atmospheric $CO_2$ levels under the baseline and $eCO_2$ SSP2-4.5 scenarios during 1950–2050.

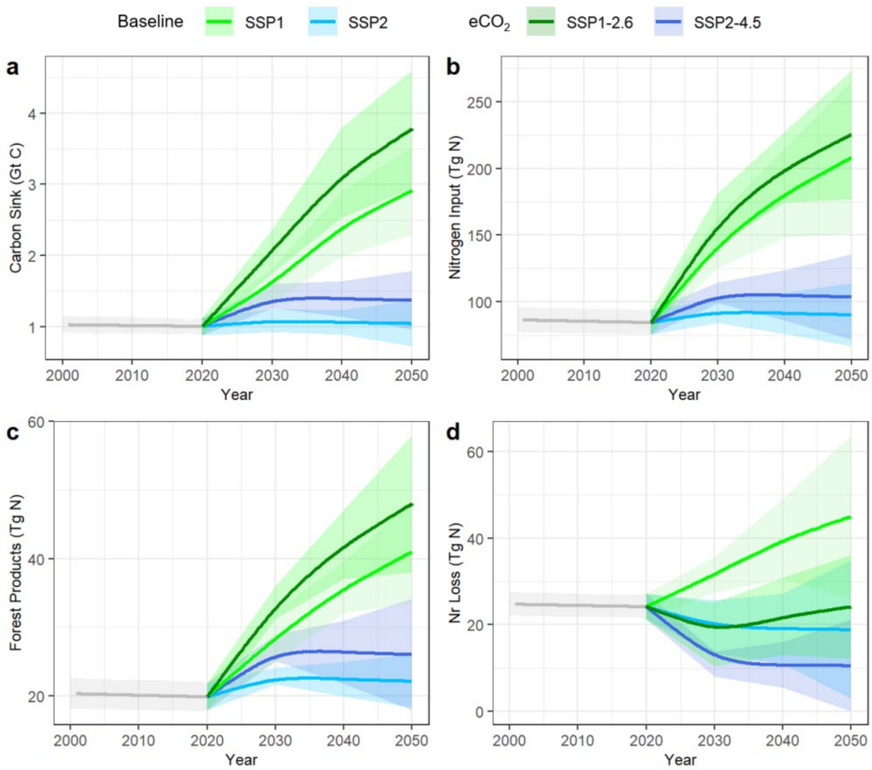


**Fig. 4 | Time series of carbon and nitrogen budgets in global forests over the period 2000-2050 under baseline and elevated $CO_2$ scenarios.** Solid lines represent mean values of carbon sink (**a**), total nitrogen input (**b**), forest products (**c**), and $N_r$ loss (**d**). Shadings represent standard deviations of the model ensembles.

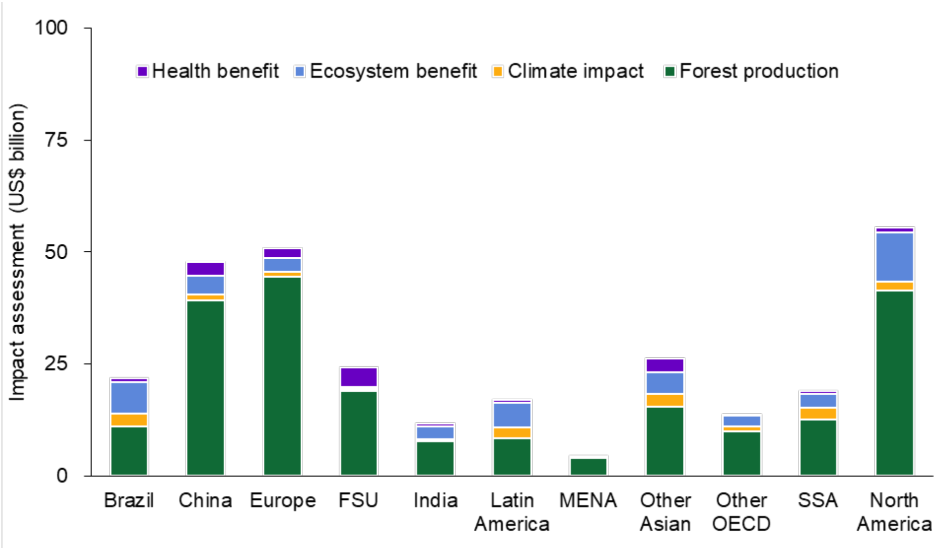


**Fig. 5 | Impact assessment of elevated atmospheric $CO_2$ levels as a single climate change factor on forests under the elevated $CO_2$ middle road scenario (SSP2-4.5) relative to the baseline in 2050.** The positive values indicate benefit. FSU, Former Soviet Union; MENA, Middle East and North Africa; OECD, Organization for Economic Cooperation and Development; SSA, Sub-Saharan Africa.

## References

1. FAO, Global forest resources assessment 2020. Rome (2020).
2. DESA, The global forest goals report 2021. New York (2021).
3. Bonan, G. B. Forests and climate change: Forcings, feedbacks, and the climate benefits of forests. *Science.* **320**, 1444–1449 (2008).
4. IPCC. *Global Warming of 1.5°C*. (2018) doi:10.1017/9781009157940.
5. Harris, N. L. *et al.* Global maps of twenty-first century forest carbon fluxes. *Nat. Clim. Chang.* **11**, 234–240 (2021).
6. Walker, W. S. *et al.* The global potential for increased storage of carbon on land. *Proc. Natl. Acad. Sci. U. S. A.* **119**, 1–12 (2022).
7. Chen, C., Riley, W. J., Prentice, I. C. & Keenan, T. F. CO2 fertilization of terrestrial photosynthesis inferred from site to global scales. *Proc. Natl. Acad. Sci. U. S. A.* **119**, (2022).
8. Ruehr, S. *et al.* Evidence and attribution of the enhanced land carbon sink. *Nat. Rev. Earth Environ.* (2023) doi:10.1038/s43017-023-00456-3.
9. Fernández-Martínez, M. *et al.* Global trends in carbon sinks and their relationships with CO2 and temperature. *Nat. Clim. Chang.* **9**, 73–79 (2019).
10. Lu, X. *et al.* Nitrogen deposition accelerates soil carbon sequestration in tropical forests. *Proc. Natl. Acad. Sci. U. S. A.* **118**, 1–7 (2021).
11. Hong, S. *et al.* Asymmetry of carbon sequestrations by plant and soil after forestation regulated by soil nitrogen. *Nat. Commun.* **14**, 1–10 (2023).
12. Luo, Y. *et al.* Progressive nitrogen limitation of ecosystem responses to rising atmospheric carbon dioxide. *Bioscience* **54**, 731–739 (2004).
13. Kou, D. *et al.* Progressive nitrogen limitation across the Tibetan alpine permafrost region. *Nat. Commun.* **11**, (2020).
14. Guo, Y. *et al.* Enhanced leaf turnover and nitrogen recycling sustain CO2 fertilization effect on tree-ring growth. *Nat. Ecol. Evol.* **6**, 1271–1278 (2022).
15. Du, E., Fenn, M. E., De Vries, W. & Ok, Y. S. Atmospheric nitrogen deposition to global forests: Status, impacts and management options. *Environ. Pollut.* **250**, 1044–1048 (2019).
16. Feng, M. *et al.* Overestimated nitrogen loss from denitrification for natural terrestrial ecosystems in CMIP6 Earth System Models. *Nat. Commun.* **14**, 1–9 (2023).
17. Koch, A. & Kaplan, J. O. Tropical forest restoration under future climate change. *Nat. Clim. Chang.* **12**, 279–283 (2022).
18. Tian, H. *et al.* Model estimates of net primary productivity, evapotranspiration, and water use efficiency in the terrestrial ecosystems of the southern United States during 1895-2007. *For. Ecol. Manage.* **259**, 1311–1327 (2010).
19. Gu, B. *et al.* Cost-effective mitigation of nitrogen pollution from global croplands. *Nature* **613**, 77–84 (2023).
20. Ainsworth, E. A. & Long, S. P. What have we learned from 15 years of free-air CO2 enrichment (FACE)? A meta-analytic review of the responses of photosynthesis, canopy properties and plant production to rising CO2. *New Phytol.* **165**, 351–372 (2005).
21. Terrer, C., Vicca, S., Hungate, B. A., Phillips, R. P. & Prentice, I. C. Mycorrhizal association as a primary control of the CO2 fertilization effect. *Science* vol. 353 72–74

(2016).
22. Cheng, W. *et al.* Global monthly gridded atmospheric carbon dioxide concentrations under the historical and future scenarios. *Sci. Data* **9**, 1–13 (2022).
23. Yu, Z. *et al.* Forest expansion dominates China's land carbon sink since 1980. *Nat. Commun.* **13**, 5374 (2022).
24. Roebroek, C. T. J., Duveiller, G., Seneviratne, S. I., Davin, E. L. & Cescatti, A. Releasing global forests from human management: How much more carbon could be stored? *Science.* **380**, 749–753 (2023).
25. Hume, A. M., Chen, H. Y. H. & Taylor, A. R. Intensive forest harvesting increases susceptibility of northern forest soils to carbon, nitrogen and phosphorus loss. *J. Appl. Ecol.* **55**, 246–255 (2018).
26. Chen, M. *et al.* Global land use for 2015–2100 at 0.05° resolution under diverse socioeconomic and climate scenarios. *Sci. Data* **7**, 1–11 (2020).
27. Zhang, J., Fu, B., Stafford-smith, M., Wang, S. & Zhao, W. Improve forest restoration initiatives to meet sustainable development goal 15. *Nat. Ecol. Evol.* (2015) doi:10.1038/s41559-020-01332-9.
28. Reich, P. B. *et al.* Even modest climate change may lead to major transitions in boreal forests. *Nature* **608**, 540–545 (2022).
29. Wu, Q. *et al.* Contrasting effects of altered precipitation regimes on soil nitrogen cycling at the global scale. *Glob. Chang. Biol.* **28**, 6679–6695 (2022).
30. Wang, J. *et al.* Precipitation manipulation and terrestrial carbon cycling: The roles of treatment magnitude, experimental duration and local climate. *Glob. Ecol. Biogeogr.* **30**, 1909–1921 (2021).
31. Shah, N. W. *et al.* The effects of forest management on water quality. *For. Ecol. Manage.* **522**, (2022).
32. Ben Keane, J. *et al.* Grassland responses to elevated CO2 determined by plant–microbe competition for phosphorus. *Nat. Geosci.* (2023) doi:10.1038/s41561-023-01225-z.
33. Tian, Y. *et al.* Long-term soil warming decreases microbial phosphorus utilization by increasing abiotic phosphorus sorption and phosphorus losses. *Nat. Commun.* **14**, 864 (2023).
34. Beck, H. E. *et al.* Present and future köppen-geiger climate classification maps at 1-km resolution. *Scientific Data* vol. 5 180214 (2018).
35. Hedges, L. V., Gurevitch, J. & Curtis, P. S. The meta-analysis of response ratios in experimental ecology. *Ecology* **80**, 1150 (1999).
36. Rosenberg, M., Adams, D. & Gurevitch, J. MetaWin: Statistical software for meta-analysis. Version 2.0. *Sinauer Assoc.* (2000).
37. Viechtbauer, W. Conducting meta-analyses in R with the metafor. *J. Stat. Softw.* **36**, 1–48 (2010).
38. Gu, B. *et al.* Toward a generic analytical framework for sustainable nitrogen management: application for China. *Environ. Sci. Technol.* **53**, 1109–1118 (2019).
39. Gu, B. *et al.* Abating ammonia is more cost-effective than nitrogen oxides for mitigating PM2.5 air pollution. *Science.* **374**, 758–762 (2021).
40. Kristal, S. L., Randall-Kristal, K. A. & Thompson, B. M. *The society for academic emergency medicine's 2004-2005 emergency medicine faculty salary and benefit*

*survey*. *Academic Emergency Medicine* vol. 13 (2006).
41. Sobota, D. J., Compton, J. E., McCrackin, M. L. & Singh, S. Cost of reactive nitrogen release from human activities to the environment in the United States. *Environ. Res. Lett.* **10**, 025006 (2015).
42. Zhang, X. *et al.* Societal benefits of halving agricultural ammonia emissions in China far exceed the abatement costs. *Nat. Commun.* **11**, 1–10 (2020).
43. Dolphin, G. & Xiahou, Q. World carbon pricing database: sources and methods. *Sci. Data* **9**, 1–7 (2022).

# Supplementary Files

This is a list of supplementary files associated with this preprint. Click to download.

- SIForestCO2.pdf